TIMING SYNCHRONIZATION IN MIMO-OFDM SYSTEMS

A thesis presented to the faculty of the Graduate School of
Western Carolina University in partial fulfillment of the
requirements for the degree of Master of Science in Technology.

By

Farhan Farhan

Director: James Z. Zhang
Professor and Dean
Department of Engineering and Technology

Committee Members: Yeqin Huang, Department of Engineering and Technology
Weiguo Yang, Department of Engineering and Technology

March 2013

To my parents Mr. & Mrs. Michael Mehboob and my love Merab Mushfiq

ACKNOWLEDGEMENTS

One cannot even imagine the power of the God that guides us all and we cannot succeed without Him. I would like to acknowledge my deepest gratitude to GOD ALMIGHTY who blessed me with the opportunity to complete this thesis project.

The completion of this research project is never complete without thanking those people who helped me to complete it. First of all I thank Dr. James Zhang my major advisor for his guidance, support, patience, trust and time during the completion of research. Without his efforts and support I would not be able to complete my research. I would like to thank Dr. Weiguo Yang and Dr. Yeqin Huang for serving as my thesis committee members. I also want to thank Dr. Aaron Ball for his help and encouragement during the research.

In the end, I wish to thank the staff members of Engineering and Technology department and Kimmel School for providing the required facilities to perform the research.

TABLE OF CONTENTS

LIST OF TABLES

LIST OF FIGURES

ABSTRACT

TIMING SYNCHRONIZATION IN MIMO-OFDM SYSTEMS

Farhan Farhan, M.S.T.

Western Carolina University (March 2013)

Director: James Z. Zhang

OFDM (Orthogonal Frequency Division Multiplexing) provides a promising physical layer for 4G and 3GPP LTE Systems in terms of efficient use of bandwidth and high data rates. It is used in several applications like WiFi (IEEE 802.11n), WiMax (IEEE 802.16), Digital Audio Broadcasting (DAB), Digital Video Broadcasting (DVB) and so on. OFDM suffers from inter-symbol interference and inter-carrier interference in wireless and fading environments and it is important to estimate and correct the start of OFDM symbol efficiently to reduce timing and frequency offset errors. Synchronization issues in OFDM are crucial and can lead to certain amount of information loss if they are not properly addressed. There are two modes of implementation forDigital Video Broadcasting-Terrestrial (DVB-T) and this thesis implements the $2K$ mode. It highlights the implementation of OFDM in DVB-T according to the European Telecommunications Standards Institute (ETSI) . It mainly focuses on the timing offset problem present in OFDM systems and its proposed solution using Cyclic Prefix (CP) as a modified Schmidl and Cox's (SC) algorithm. Simulations were performed to compare the different synchronization methods with different amount of timing offsets and under different channel environments.

CHAPTER 1: INTRODUCTION

This chapter reviews the history and architecture of OFDM. Section 1.1 explains the history of multicarrier systems and the evolution of Orthogonal Frequency Division Multiplexing (OFDM). Section 1.2 explains the detail of OFDM transmitter and receiver. It also explains the other blocks of an OFDM system. The limitations and drawbacks associated with OFDM has been explained in section 1.3. The applications of the OFDM are reviewed in section 1.4 whereas section 1.5 reviews the different wireless, digital video and audio standards.

1.1 History

The advancement in wireless and mobile communication has led the researchers to design and implement transceiver with higher data rates using the bandwidth efficiently. The single carrier modulation scheme is not enough to meet the demands of high data rates and higher capacity. To achieve this goal, multicarrier networks such as Frequency Division Multiplexing (FDM) were utilized since 1950's but it was hard to implement those networks. This implementational complexity caused to limit their use for military applications [1] . In a multicarrier system, there are a number of carriers which carry the information in parallel manner. This system is less susceptible to noise and interference especially in wireless environment. Chang [2] was the first who introduced OFDM by further developing and utilizing the Frequency Division Multiplexing (FDM) in 1950.

1.2 Orthogonal Frequency Division Multiplexing (OFDM)

Orthogonal Frequency Division Multiplexing is a digital Multi-carrier modulation scheme in which a large number of closely spaced orthogonal subcarriers are used to carry the data [3].

The data is divided into several parallel data streams or channels, one for each sub-carrier. Each sub-carrier is modulated with a conventional modulation scheme such as M-ary Phase Shift Keying (M-PSK) or Quadrature Amplitude Modulation (QAM) at a low symbol rate, maintaining total data rates similar to those in a conventional single-carrier modulation scheme in the same bandwidth.

1.2.1 Structure of OFDM

This section describes the transmitter, receiver and other blocks of OFDM system [4]. The block diagram of OFDM transceiver is shown in the Figure 1.1.

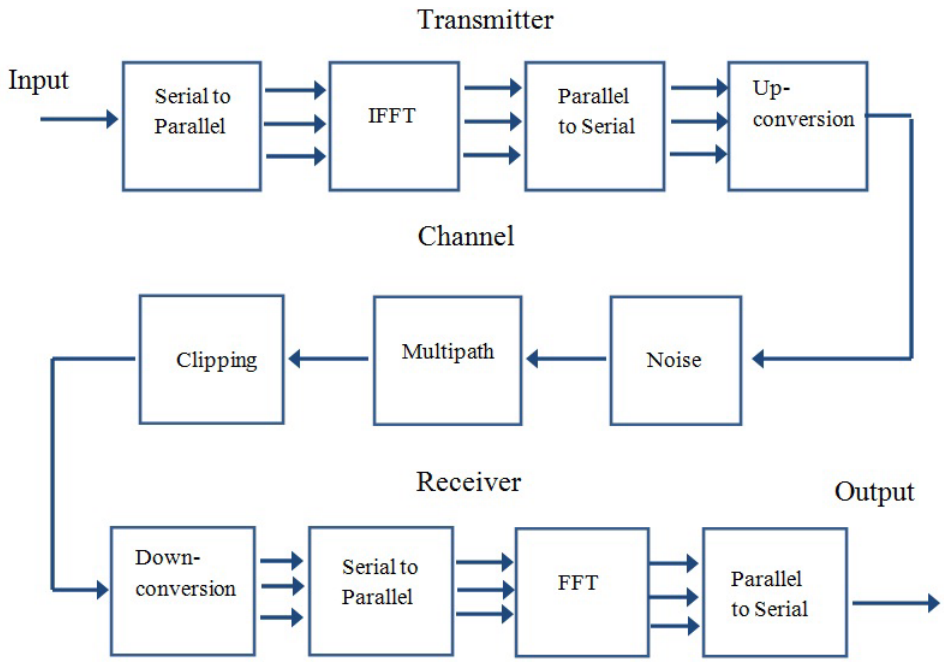

Figure 1.1: Structure of OFDM System

Transmitter

In a conventional OFDM transmitter [5], serial stream of data is first generated. This serial data is then mapped to the complex symbols using different constellation mapping either Phase Shift Keying or Quadrature Amplitude Modulation. After mapping to different complex symbols, the serial data is converted into parallel streams of data using a serial to parallel block (S/P). We use Inverse Fast Fourier Transform (IFFT) to modulate the parallel data stream. After performing IFFT, the data is again converted into serial stream using the parallel to serial block (P/S).

This process in the transmitter [6] gives the passband OFDM signal after up-conversion to be transmitted.

Cyclic Prefix (CP)

The OFDM transceiver has a block named Cyclic Prefix (CP) or Guard Interval (GI) which is appended at the start of the serial stream at the baseband before up-converted to passband frequency. The cyclic Prefix is actually an exact copy of the last part or samples of the data. The purpose of CP is to remove the Inter-symbol Interference (ISI) and channel effects. The drawback of cyclic prefix is that it is redundant and requires extra power to transmit along with the OFDM symbol whose effect appears in Signal to Noise Ratio (SNR).

Channel

After upconversion of the baseband OFDM signal into passband OFDM signal, it is transmitted over the channel. The channel is important if we want to investigate the system performance over the physical layer. There are several types of channel distributions and have different channel characteristics. The one very important channel model is Additive White Gaussian Noise (AWGN) channel but in the practical situation, most of the time the signal encounters multipath, frequency selective fading channels like Rayleigh or Rician Channel and therefore AWGN channel is not good if we want to analyze the system performance over the terrestrial link where signal will have to face multipath, interference, and non-linearity [7]. But it is a very good model to investigate the system behavior in general.

Receiver

The receiver [8] in OFDM system is exactly the reverse of transmitter. At the receiver side, the signal is first down-converted to baseband signal. After removing CP from the received data, it is converted into parallel streams of data using the serial to parallel block. Then we perform Fast Fourier Transform (FFT) of the data. The data is then converted into serial data and then decoded to retrieve the information. We also perform the some synchronization algorithms to

remove the synchronization errors at the receiver side.

1.2.2 Theory of OFDM

Orthogonality

Orthogonality in sub-carriers is one of the most important characteristics of OFDM. This makes OFDM sub-carriers to overlap each other in frequency domain having efficient use of available bandwidth. As described in [9], two time limited complex exponential signals will be orthogonal if

$$\frac{1}{T_{sym}} \int_0^{T_{sym}} e^{j2\pi f_k t} e^{-j2\pi f_i t} \mathrm{dt} = \begin{cases} 1, & \forall \text{ integer } k{=}i \\ 0, & \text{otherwise} \end{cases} \tag{1.1}$$

Where T_{sym} is the OFDM symbol duration. f_k and f_i represent different subcarrier frequencies respectively.

It is an important to ensure that an OFDM system remains Inter-Carrier Interference (ICI) free [3]. ICI degrades the system performance but the feature of orthogonality provides the guarantee for the system to be ICI free.

OFDM Modulation and Demodulation

After encoding data and mapping it to the constellation symbols, it is converted into parallel streams using serial to parallel converter. Consider $X_m[k]$ be the m^{th} transmit symbol at the k^{th} sub-carrier. Let $\Psi_{m,k}(t)$ be the m^{th} OFDM symbol at k^{th} sub-carrier [9], given by:

$$\Psi_{m,k}(t) = \begin{cases} e^{j2\pi f_k (t - mT_{sym})}, & 0 < t \leq T_{sym} \\ 0, & elsewhere \end{cases} \tag{1.2}$$

Similarly, the continuous-time domain OFDM baseband signal can be written as:

$$x_m(t) = \sum_{m=0}^{\infty} \sum_{k=0}^{N-1} X_m[k] e^{j2\pi f_k (t - mT_{sym})} \tag{1.3}$$

where $X_m[k]$ is the m^{th} transmitted symbol at k^{th} sub-carrier.
The baseband discrete-time OFDM signal will be written as:

$$x_m[n] = \sum_{k=0}^{N-1} X_m[k] e^{j2\pi kn/N} \text{ for } n = 0, 1, 2, ..., N-1 \tag{1.4}$$

where N is the total number of samples.
As it can be observed that equation (1.4) represents the Inverse Discrete Fourier Transform (IDFT) of $X_m[k]$. IDFT can be calculated efficiently by IFFT algorithms therefore there are IFFT and FFT blocks in the block diagram to perform the operations of IDFT and DFT, respectively.
The above equation was obtained by sampling the continuous-time baseband OFDM signal at $t = mT_{sym} + nT_s$ with $T_s = \frac{T_{sym}}{N}$.

Consider the received baseband OFDM symbol $y_m(t) = \sum_{k=0}^{N-1} X_m[k] e^{j2\pi f_k (t - mT_{sym})}$ with $mT_{sym} < t \leq mT_{sym} + nT_s$. The transmitted baseband OFDM signal $X_m[k]$ can be reconstructed using the orthogonality among the sub-carriers. The transmitted OFDM signal was reconstructed without taking the effect of channel and noise [9]. The process is shown in discrete-time domain as follows:

$$
\begin{aligned}
Y_m[k] &= \sum_{n=0}^{N-1} y_m[n] e^{-j2\pi kn/N} \\
&= \sum_{n=0}^{N-1} \{\frac{1}{N} \sum_{i=0}^{N-1} X_m[i] e^{j2\pi in/N}\} e^{-j2\pi kn/N} \\
&= \frac{1}{N} \sum_{n=0}^{N-1} \sum_{i=0}^{N-1} X_m[i] e^{j2\pi(i-k)n/N} = X_m[k]
\end{aligned}
\tag{1.5}
$$

1.3 Limitations and Drawbacks of OFDM

Though OFDM is very useful and it has made it possible to use bandwidth efficiently. However, it has some serious drawbacks which causes loss of information if they are not corrected in the system. These errors include Timing Offsets, Carrier Frequency Offsets (CFO) and Non-linearities. This section explains the above errors and their effects on the performance of OFDM. As referenced in [9] and [10], the details of these errors are eplained as follows.

Timing Offset Error

In OFDM, modulation and demodulation are accomplished using IFFT and FFT techniques which cause delay in the system. It is important to find the start of the OFDM symbol at the receiving end and the error in estimating the beginning of symbol causes the timing offset error. Therefore it is necessary to perform symbol time synchronization to accurately locate the start of the OFDM symbol. If this delay is not corrected, it causes phase rotation in the constellation. Let δ be the amount of offset in time domain, it causes a phase offset of $2\pi k\delta/N$ in the frequency domain. This phase offset varies directly in proportion to the sub-carrier index k [9].

Consider the received signal in time-domain with the timing offset already introduced in it, i.e., $x[n+\delta]$, then the FFT of that signal is:

$$
\begin{aligned}
Y_m[k] &= \frac{1}{N}\sum_{n=0}^{N-1} x_m[n+\delta]e^{-j2\pi nk/N} \\
&= \frac{1}{N}\sum_{n=0}^{N-1}\{\sum_{i=0}^{N-1} X_m[i]e^{j2\pi(n+\delta)i/N}\}e^{-j2\pi nk/N} \\
&= \frac{1}{N}\sum_{i=0}^{N-1} X_m[i]e^{j2\pi i\delta/N}\sum_{n=0}^{N-1} e^{j2\pi\frac{i-k}{N}n} \\
&= X_m[k]e^{j2\pi k\delta/N}
\end{aligned}
\tag{1.6}
$$

The above expression (1.7) shows that sub-carrier frequency components remain orthogonal but the phase offset term causes the rotation in signal constellation.

Carrier Frequency Offset

Carrier Frequency Offset is the amount of offset introduced by the mismatch in the frequency of transmitter and receiver local oscillator (LO), non-linear channels and Doppler shifts [11]. The type of carrier distortion introduced by the non-linearities of the channels is phase noise whereas CFO is the one produced by Doppler Shifts [9]. Synchronization of CFO correction is necessary to avoid loss of orthogonality in sub-carriers. As referenced in [9], consider carrier frequencies at transmitter and receiver as f_c and $f_c^{'}$. Suppose that f_o is the offset frequency obtained by taking the difference of f_c and $f_c^{'}$. Let ε be the normalized CFO defined as:

$$
\varepsilon = \frac{f_o}{\Delta f} = \frac{f_c - f_c^{'}}{\Delta f} \tag{1.7}
$$

where Δf is the sub-carrier spacing.

CFO has two parts namely integer CFO and fractional CFO. If ε_i is the integer part and ε_f is the fractional part of CFO, then

$$\varepsilon = \varepsilon_i + \varepsilon_f \tag{1.8}$$

It is important to note that CFO causes a phase rotation of $2\pi n\varepsilon$ for an OFDM signal in time-domain and it is equivalent to a frequency shift of amount $-\varepsilon$ for OFDM signal in frequency-domain.

Peak to Average Power Ratio (PAPR)

Another problem that OFDM has is the Peak to Average Power Ration (PAPR). After the operation of IFFT (which adds the N sinusoids) at the transmitter side, large peaks are produced by some of the combinations of sinusoids. These large peaks make it difficult for the design in terms of IFFT or FFT wordlength, DAC or ADC and High Power Amplifier (HPA). The saturation at HPA occurs due to these large peaks which causes in and out of band distortion [12]. By definition, the PAPR is given by the ratio of maximum peak power divided by the average power of the OFDM signal. There are several techniques proposed in the today's literature to reduce the PAPR of OFDM signals [13].

1.4 Applications and uses of OFDM

OFDM finds its use in many applications [14] in the field of wireless communication. With specific design guidelines, it is used in Mobile and fixed Wireless Systems, Ultra-wide Band (UWB) Systems and Cognitive Radio. OFDM has been adopted in IEEE 802.16 standards [15] to aid data rate up to 75 Mbps at the frequency bands under 11 GHz. OFDM is used in the downlink of 3GPP LTE as modulation technique. OFDM is also used in Digital Audio Broadcasting and Digital Video Broadcasting.

1.5 Wireless Standards

There are several different standards for wireless communication systems. Two main standards are WiMAX and WiFi.

1.5.1 WiMAX (IEEE 802.16 family of Standards)

Worldwide Interoperability for Microwave Access (WiMAX)) is a telecommunications protocol that provides fixed and fully mobile Internet access [16] . The current WiMAX revision provides up to 40 Mbps with the IEEE 802.16m update expected to offer up to 1 Gbps fixed speeds. The WiMAX nomenclature was introduced by the WiMAX Forum, an industry consortium, to promote the Institute of Electrical and Electronics Engineers (IEEE) 802.16 family of standards for broadband wireless access systems. The early iterations of IEEE 802.16 focused on line-of-sight (LOS) applications using high-frequency bands between 10 to 66 GHz. More recently, efforts have been focused on specifying amendments to the early standards to support non-line-of-sight (NLOS) applications between 2 to 11 GHz. The 802.16-2004 standard, more commonly known as 802.16d, was published in 2004. The 802.16e standard is an amendment to the 802.16d standard and was ratified at the end of 2005 and published as 802.16-2005. While the 802.16d standard supports fixed and nomadic applications, the 802.16e standard supports fixed, nomadic, portable and mobile solutions [17].

IEEE 802.16d

It is sometimes referred to as '$FixedWiMAX'$, since it has no support for mobility. The Fixed WiMAX IEEE 802.16d standard supports both Time Division Duplex (TDD) and Frequency Division Duplex (FDD) services. The latter of which is far more popular with mobile wireless providers than the newer TDD approach.

IEEE 802.16e

IEEE 802.16e is an amendment to IEEE 802.16d. It introduced support for mobility and is therefore also known as 'Mobile WiMAX'. Mobile WiMAX is the WiMAX incarnation that is of most commercial interest to date and is being actively deployed in many countries. Mobile WiMAX is also the basis of future revisions of WiMAX. The IEEE 802.16 standard essentially standardizes two aspects of the air interface - the physical layer (PHY) and the Media Access Control layer (MAC). This section provides an overview of the technology employed in these two layers in the mobile IEEE 802.16e specification.

• **PHY**

IEEE 802.16e uses Scalable OFDMA to carry data, supporting channel bandwidths between 1.25 MHz and 20 MHz, with up to 2,048 sub-carriers. It supports adaptive modulation and coding, so that in benign channels, a highly efficient 64-QAM coding scheme is used, whereas when the channel is bad, a more robust BPSK coding mechanism is used. In intermediate conditions, 16-QAM and QPSK can also be employed. Other PHY features include support for multiple antennas, i.e., a Multiple-In Multiple-Out (MIMO) system in order to provide good NLOS characteristics (or higher bandwidth) and Hybrid Automatic Repeat request (HARQ) for good error correction performance.

• **MAC**

The IEEE 802.16 MAC describes a number of Convergence Sublayers which describe how wireline technologies such as Ethernet, ATM and IP are encapsulated on the air interface, and how data is classified, etc. It also describes how secure communications are delivered, by using secure key exchange during authentication, and encryption using AES or DES (as the encryption mechanism) during data transfer. Further features of the MAC layer include power saving mechanisms (using Sleep Mode and Idle Mode) and handover mechanisms.

1.5.2 WiFi (IEEE 802.11 family of Standards)

The original version of the IEEE 802.11 standard was released in 1997 and adopted in 1999, but is today obsolete. It specified two net bit rates of 1 or 2 Mbps, plus forward error correction.

It specified three alternative physical layer technologies: diffuse infrared operating at 1 Mbps; frequency-hopping spread spectrum operating at 1 Mbps or 2 Mbps; and direct-sequence spread spectrum operating at 1 Mbps or 2 Mbps. The latter two radio technologies used microwave transmission over the Industrial Scientific and Medical (ISM) frequency band located at 2.4 GHz [18]. Legacy IEEE 802.11 with direct-sequence spread spectrum was rapidly supplanted and popularized by IEEE 802.11b.

IEEE 802.11a

The IEEE 802.11a standard uses the same data link layer protocol and frame format as the original standard, but an OFDM based air interface (physical layer). It operates in the 5 GHz band with a maximum net data rate of 54 Mbps. Since the 2.4 GHz band is heavily used utilizing the relatively unused 5 GHz band gives 802.11a a significant advantage.

IEEE 802.11b

IEEE 802.11b has a maximum raw data rate of 11 Mbps and uses the same media access method defined in the original standard. IEEE 802.11b products appeared in the market in early 2000, since IEEE 802.11b is a direct extension of the modulation technique defined in the original standard. The dramatic increase in throughput of IEEE 802.11b devices (compared to the original standard) along with simultaneous substantial price reductions led to the rapid acceptance of IEEE 802.11b as the definitive wireless LAN technology. IEEE 802.11b devices suffer interference from other products operating in the 2.4 GHz band. Devices operating in the 2.4 GHz range include: microwave ovens, Bluetooth devices, baby monitors and cordless telephones.

IEEE 802.11g

A third modulation standard was ratified as IEEE 802.11g in June 2003. The system works in the 2.4 GHz band, but uses the same OFDM based transmission scheme as IEEE 802.11a. IEEE 802.11g hardware is fully backwards compatible with IEEE 802.11b hardware and therefore is

encumbered with legacy issues that reduce throughput when compared to 802.11a by 21%. IEEE 802.11g standard was rapidly adopted by consumers starting in January 2003, well before ratification, due to the desire for higher data rates as well as reductions in manufacturing costs. By summer 2003, most dual-band 802.11a/b products became dual-band/tri-mode, supporting a and b/g in a single mobile adapter card or access point. Details of making b and g work well together occupied much of the lingering technical process; in an 802.11g network, however, activity of an 802.11b participant will reduce the data rate of the overall 802.11g network.
Like 802.11b, 802.11g devices suffer interference from other products operating in the 2.4 GHz band.

IEEE 802.11n

IEEE 802.11n is a recent amendment which improves upon the previous 802.11 [19] standards by adding MIMO and many other newer features. IEEE ratified the 802.11n as standard in September 2009. It defines modification to both 802.11 physical and medium access control layer. This modification was provided to achieve higher throughput, with a maximum of throughput achieved to 100 Mbps. This type of network provides anytime access, optimum performance for mobile users, coverage for RF environments and reliable connections.

CHAPTER 2: LITERATURE SURVEY

This chapter reviews the timing correction techniques and different approaches proposed in literature in the field of OFDM synchronization. Following are the different timing synchronization algorithms detailed in the respective sections.

2.1 Schmidl and Cox's Timing Algorithm

This method relies on the training sequence which has two identical halves in the time-domain and remains the same after passing through the channel. However, there is a phase difference introduced in them due to the carrier frequency offset. This algorithm used Pseudo-Noise (PN) sequence to generate two identical halves in time domain by transmitting PN sequence on even frequencies and zeros on the odd frequencies. The second training symbol has two different PN sequences on both odd and even frequencies. The reason for using the PN sequence at odd frequency is to measure the subchannels and at even frequency to determine the frequency offset. At the receiver side, the correlation between the OFDM signal and known transmitted training sequence is computed by using a window of L samples. This window slides along in time to search for the first training symbol by the means of correlation. This algorithm gives the timing metric as the result of correlation product normalized by the energy for the second half-symbol. The metric reaches a plateau when the window of L samples completely overlaps the first training symbol and the start of the OFDM frame can be taken anywhere in the spread of that plateau. As given in the reference [10], the timing metric for OFDM signal with 1000 subcarriers, a carrier spacing of 12.4 MHz, and a signal-to-noise ratio (SNR) of 10 dB is shown in the Figure 2.1.

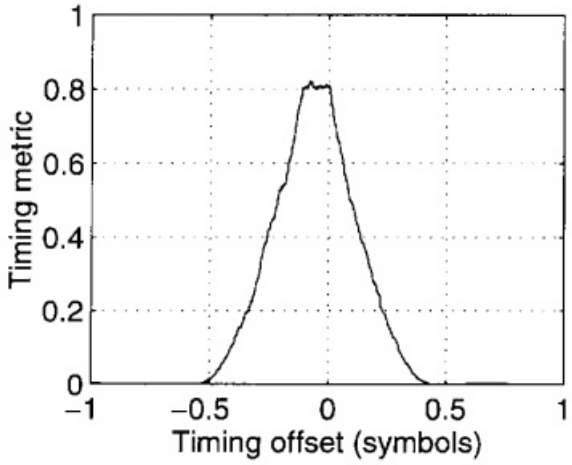

Figure 2.1: Example of Schmidl and Cox's Timing Metric

Performance Analysis of Timing Estimator

There are two factors to consider when evaluating timing estimator. The first one is to miss a training sequence and not detecting the signal or detecting a false sequence when there is no signal present. The second is the degradation when the timing estimate deviates from the correct timing.

Statistical Distribution

Suppose each complex sample r_l is expressed as the combination of signal and noise component.

$$r_l = x_l + n_l \tag{2.1}$$

Define the variance of real and imaginary parts as:

$$E[Re\{x_l\}^2] = E[Im\{x_l\}^2] = \sigma_x^2 \tag{2.2}$$
$$E[Re\{n_l\}^2] = E[Im\{n_l\}^2] = \sigma_n^2$$

Then the SNR can be defined as σ_x^2/σ_n^2. The next step is to find the mean and variance of the estimator at the best timing. To achieve this goal, consider cross-correlation '$P(d)$' as:

$$\begin{aligned} P(d) &= \sum_{l=0}^{L-1} (x_{d+l+L} + n_{d+l+L})(x_{d+l} + n_{d+l})^* \\ &= \sum_{l=0}^{L-1} x_{d+l}^* x_{d+l+L} + x_{d+l}^* n_{d+l+L} + x_{d+l+L} n_{d+l}^* + n_{d+l}^* n_{d+l+L} \end{aligned} \tag{2.3}$$

where d is the timing index and $P(d)$ is the cross-correlation of the received samples.
Let $d_{optimal}$ represent the optimal timing index and at this correct timing $P(d)$ can be written as:

$$\begin{aligned} |P(d_{optimal})| \approx e^{-j\phi} \sum_{l=0}^{L-1} x_{d_{optimal}+l}^* x_{d_{optimal}+l+L} + \sum_{l=0}^{L-1} inPhase_\phi\{x_{d_{optimal}+l}^* n_{d_{optimal}+l+L} + \\ x_{d_{optimal}+l+L} n_{d_{optimal}+l}^* + n_{d_{optimal}+l}^* n_{d_{optimal}+l+L}\} \end{aligned} \tag{2.4}$$

where $inPhase_\phi\{.\}$ is the in-phase component in the ϕ direction. As referenced in [10], $|P(d_{optimal})|$ is Gaussian with mean $2L\sigma_x^2$. Similarly auto-correlation '$R(d_{optimal})$' can be written as:

$$\begin{aligned} R(d_{optimal}) = \sum_{l=0}^{L-1} [(|x_{d_{optimal}+l+L}| + inPhase_{s_{d_{optimal}+l+L}}\left\{n_{d_{optimal}+l+L}\right\})^2 + \\ (quadrature_{s_{d_{optimal}+l+L}}\left\{n_{d_{optimal}+l+L}\right\})^2] \end{aligned} \tag{2.5}$$

$R(d_{optimal})$ is also Gaussian with mean $2L(\sigma_x^2 + \sigma_n^2)$.

2.2 Minn and Bhargava's Approach

Minn and Bhargava [20] introduced two synchronization approaches to correct timing offset by modifying the Schmidl and Cox's algorithm. The one approach used was to modify the pattern of training sequence and the other was to use the sliding window method over the one whole symbol period rather than half symbol period. In sliding window approach, the concept of averaging over 90% points was not used rather timing metric was averaged over the length of window samples N_g+1 and N_g is the number of samples in guard interval. In the method of using training sequence, the pattern used was [-A -A A A] without cyclic prefix. *A* represents the samples of length $L = \frac{N}{4}$ generated by taking the $N/4$ point IFFT of the modulated PN-sequence. In Minn and Bhargava's approach, the channel used was Additive White Gaussian Noise but the fading and multipath environments were not considered. The timing metric defined by Minn and Bhargava using the Sliding window method is given as:

$$\Lambda_1(d) = \frac{1}{N_g + 1} \sum_{k=-N_g}^{0} \Lambda_f(d+k) \tag{2.6}$$

where $\Lambda_1(d)$ is the average of timing metric $\Lambda_f(d)$.
where Minn and Bhargava's timing metric '$\Lambda_f(d)$' can be calculated as:

$$\Lambda_f(d) = \frac{|P(d)|^2}{R_f^2(d)} \tag{2.7}$$

and

$$R_f(d) = \frac{1}{2}\sum_{m=0}^{N-1} |r(d+m)|^2 \tag{2.8}$$

Where $r(k)$ is the received sample and $R_f(d)$ is the auto-correlation.
$P(d)$ is taken from the Schmidl and Cox's method and is defined as:

$$P(d) = \sum_{m=0}^{L-1} r^*(d+m)r(d+m+L) \tag{2.9}$$

Similarly, the timing metric defined in Training Symbol method is the same as $\Lambda_1(d)$ but the difference is in the definition of $P(d)$ and $R(d)$. It is defined as:

$$\Lambda_2(d) = \frac{|P_2(d)|^2}{R_2^2(d)} \tag{2.10}$$

The cross-correlation between the positive and negative parts of the sequence [20] is given by $P_2(d)$ as:

$$P_2(d) = \sum_{k=0}^{1}\sum_{m=0}^{L-1} r^*(d+2Lk+m)r(d+2Lk+m+L) \tag{2.11}$$

and auto-correlation is given by as:

$$R_2(d) = \sum_{k=0}^{1} \sum_{m=0}^{L-1} |r(d+m+2Lk+L)|^2 \tag{2.12}$$

2.3 Classen et al. Approach to Timing Synchronization

Classen [21] introduced two different timing correction techniques for coarse and fine timing, respectively. In this paper, channel impulse response (cir) was used to achieve frame synchronization as fine timing. In coarse timing, both timing and frequency offset were unknown and the approach of periodic structure was used to find the start of the symbol. This was accomplished by minimizing the metric $\hat{\delta}$ defined by the equation:

$$\hat{\delta} = argmin \left\{ \sum_{i=\delta}^{N_g-1+\delta} (|r_l[n+i]| - |r_l^*[n+N+i]|)^2 \right\} \tag{2.13}$$

where r_l is the received l^{th} sample and δ is the amount of time offset.

In fine time offset correction, it was assumed that CFO estimation and correction have been made. Mainly this technique used the information of cir to obtain timing offset correction. The technique was to consider the energy maximization of cir within interpolation window. This technique causes the energy of channel estimate to get maximized. Since interpolation adds no additional information so the metric was evaluated at the pilot positions.

2.4 Park et al. approach to Timing Synchronization

This method was proposed in modification of Schmidl and Cox's method and Minn and Bhargava's method to remove the deficiency found in timing estimator. It was achieved by changing the pattern of training sequence and the pattern of the training sequence is given by:

$$P = [x_{N/4}\ \ y^*_{N/4}\ \ x_{N/4}\ \ y^*_{N/4}] \tag{2.14}$$

where $x_{N/4}$ represents the samples of length $N/4$ generated by IFFT of PN-sequence and $y^*_{N/4}$ is the conjugate of $x_{N/4}$.

The metric defined in this method is given as:

$$\Lambda_P(d) = \frac{|P_3(d)|^2}{(R_3(d))^2} \tag{2.15}$$

where $P_3(d)$ is the cross-correlation sequence and $R_3(d)$ represents the auto-correlation sequence. Both cross-correlation and auto-correlation are given in (2.16) and (2.17), respectively:

$$P_3(d) = \sum_{k=0}^{N/2} r(d-k)r(d+k) \tag{2.16}$$

$$R_3(d) = \sum_{k=0}^{N/2} |r(d+k)|^2 \tag{2.17}$$

The estimation of timing happens at the desired correct symbol timing and the rest of the values of mutual product are zero but this timing synchronization algorithm is very sensitive to indoor multipath and AWGN channels.

CHAPTER 3: PROPOSED APPROACH AND METHODOLOGY

3.1 Implementation of DVB-T (Digital Video Broadcasting-Terrestrial) using OFDM

The block diagram for DVB-T standard is shown in the Figure 3.1. The processes described in this diagram are carried out in a Digital Signal Processor (DSP). This section focuses on the implementation of 2K mode of DVB-T standard and the parameters for this mode are given in table 3.1.

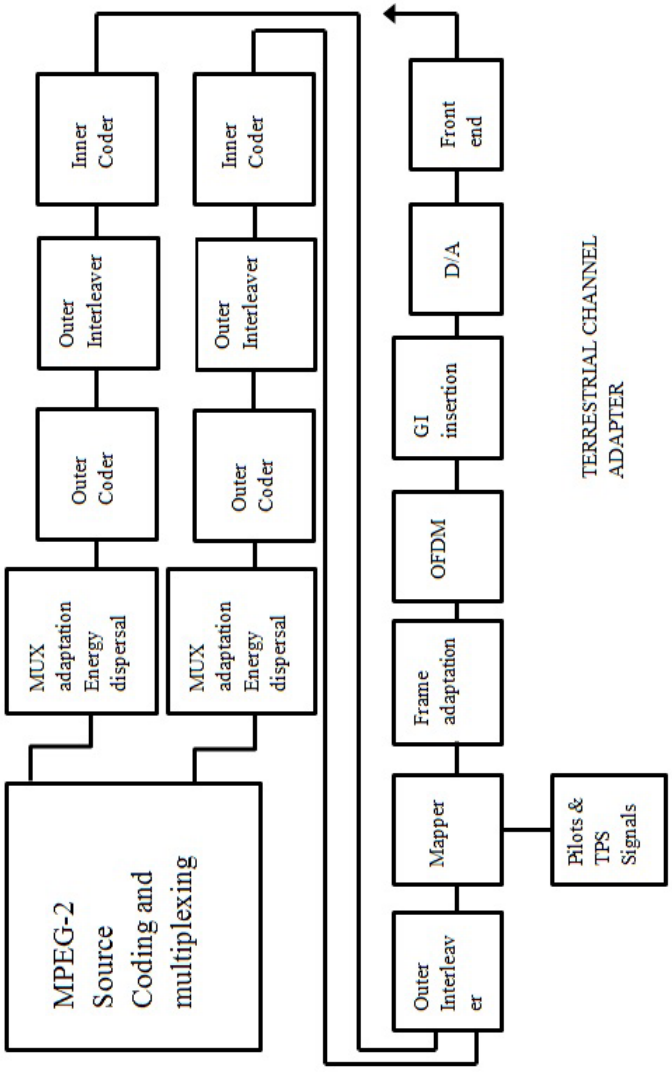

Figure 3.1: Block Diagram for DVB-T Transmitter

Table 3.1: OFDM Parameters for DVB-T 2K mode

Parameter	2K mode
Elementary Period (T)	7/64 μs
Number of carriers (K)	1705
Value of carrier number K_{min}	0
Value of carrier maximum K_{max}	1704
Duration (T_U)	224μs
Carrier Spacing ($\frac{1}{T_U}$)	4,464 Hz
Spacing between carriers K_{min} and K_{max} ($\frac{K-1}{T_U}$)	7.61 MHz
Allowed guard interval $\frac{\Delta}{T_U}$	1/4 | 1/8 | 1/16 | 1/32
Duration of symbol part T_U	224μs
Duration of gaurd interval Δ	56μs | 28μs | 14μs | 7μs
Symbol duration $T_s = \Delta + T_U$	280μs | 252μs | 238μs | 231μs

The OFDM signal expression in DVB-T is given by the following emitted signal

$$x(t) = Re\left\{ e^{j2\pi f_c t} \sum_{m=0}^{\infty} \sum_{l=0}^{67} \sum_{k=k_{min}}^{k_{max}} c_{m,l,k} \Psi_{m,l,k}(t) \right\} \tag{3.1}$$

where:

$$\Psi_{m,l,k}(t) = \begin{cases} e^{j2\pi \frac{k'}{T_U}(t-\Delta-l\times T_s-68\times m\times T_s)}, & (l+68\times m)\times T_s \\ \leq t \leq (l+68\times m+1)\times T_s & \\ 0, & elsewhere \end{cases} \tag{3.2}$$

where:

k denotes the carrier number;

l denotes the OFDM symbol number;

m denotes the transmission frame number;

K is the number of transmitted carriers;

T_s is the symbol duration;

T_U is the inverse of the carrier spacing;

Δ is the duration of the guard interval;

f_c is the central frequency of the radio frequency (RF) signal;

$k^{'}$ is the carrier index relative to the center frequency, $k^{'} = k - (K_{max} + K_{min})/2$

$c_{m,0,k}$ complex symbol for carrier k of the Data symbol no.1 in frame number m;

$c_{m,1,k}$ complex symbol for carrier k of the Data symbol no.2 in frame number m;

...

$c_{m,67,k}$ complex symbol for carrier k of the Data symbol no.68 in frame number m

3.1.1 OFDM Frame Structure in DVB-T 2K Mode

The 2K mode of DVB-T is specifically for the mobile reception of standard definition DTV (Digital Television). The OFDM transmission is carried out in frames. Each frame has a duration of T_F and consists of 68 OFDM symbols [22]. One super-frame consists of four frames and each symbol is comprised of 1705 carriers in 2K mode with T_s as the symbol duration. It is composed of two parts: a useful part with duration T_U and a guard interval with a duration Δ. The guard interval consists in a cyclic continuation of the useful part, T_U, and is inserted before it. There are four values of guard intervals that can be used as defined in [23]. The symbols in OFDM are numbered from 0 to 67. All the symbols have data and reference information. There are standards only for DVB-T transmitter and the design of receiver is open.

3.1.2 OFDM Transmission and Reception in DVB-T

A block diagram of the generation of OFDM symbol is shown in the Figure 3.2. The approach is similar to what was done in [24] and the only difference was the addition of timing jitter and different distribution of physical channels. The addition of timing offset, physical channel distributions and performance analysis made it more realistic and practical. In the implementation, it was important to consider the appropriate simulation time and in order to fulfill Nyquist criterion, simulation period was kept related to elementary period T. $R_s = 40/T$ was used as the relation between simulation period and elementary period which gave carrier frequency nearly

equal to 90MHz. The centering of OFDM spectrum at carrier frequency was achieved by using the 2N-IFFT [24] and T/2 as elementary period.

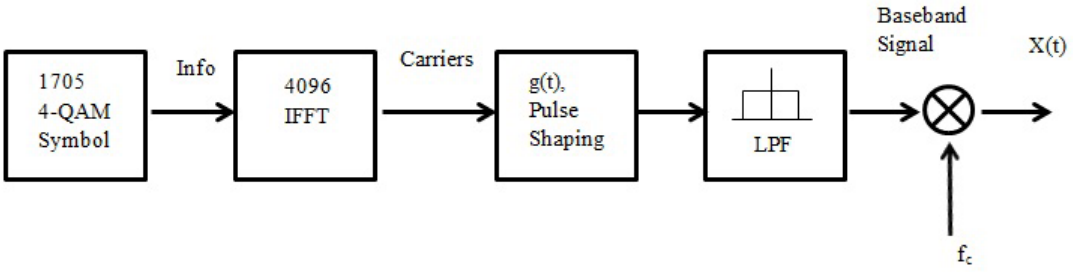

Figure 3.2: OFDM symbol generation

Similarly, the block diagram for the reception of OFDM symbol is straight opposite of generation of OFDM symbol. The block diagram is shown in the figure 3.3.

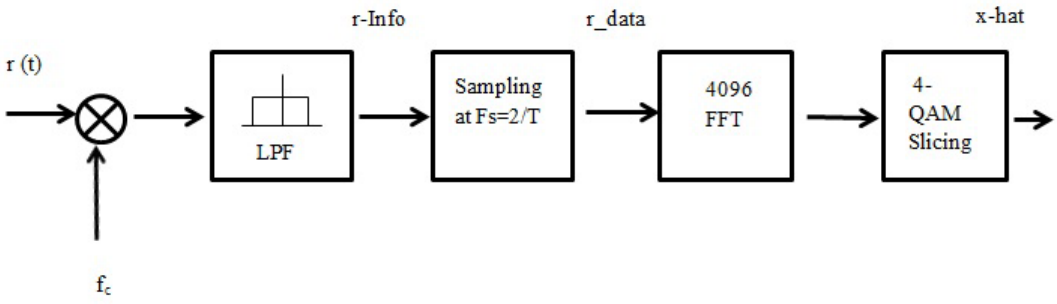

Figure 3.3: OFDM Symbol Reception

3.2 Timing Synchronization and Proposed Approach

There are several methods to address the issue of timing offset correction in literature. Classen focused on a method to find both timing offset and carrier frequency offset together. In his

method, he considered the trial and error method which was very computationally complex [21]. Another way to find the timing offset is using the means of slopes of the curve of carrier phases in pilots versus the index of pilots.Minn and Bhargava presented the timing synchronization by modifying the Schmidl and Cox's method and using a new pattern for training sequence [20]. This paper provides the modified Schmidl and Cox's approach by not using the training sequence and making cyclic prefix (CP) as the reference. It does not normalize the correlation metric as it was done in Schmidl and Cox's algorithm. The main advantage of avoiding training sequence is to obtain efficiency in transmitting power. The methods which require the use of training preamble require extra overhead for transmitting training sequences along with the information signal. This approach uses the sliding window technique to compute the correlation of the received signal with the cyclic prefix which is already known to the user. The timing metric obtained by the correlation shows the variance and the start of OFDM frame can be taken where the maximum lies in this spread of variance. A comparison of some different synchronization schemes as described in literature survey was performed and those results as well as the proposed approach are shown in the following figures.

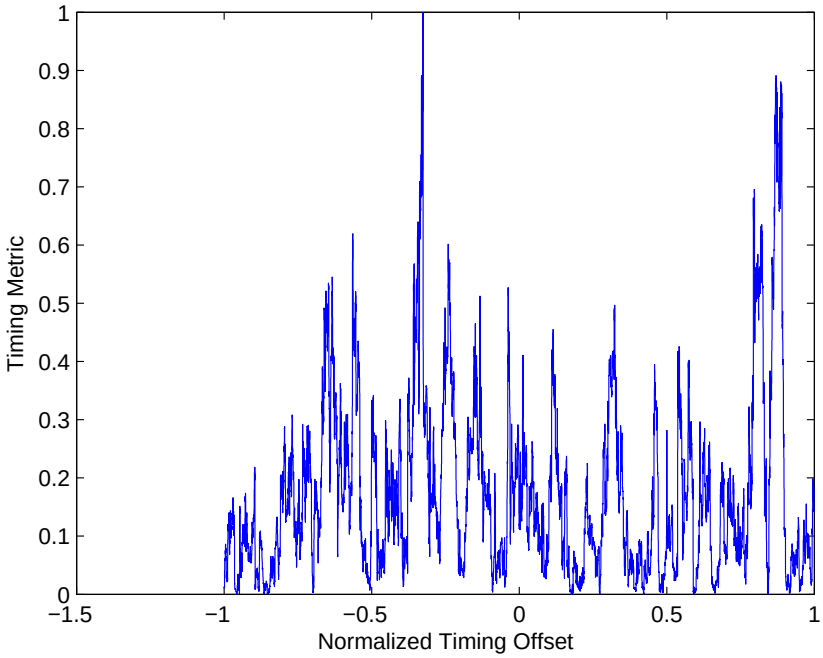

Figure 3.4: Proposed Approach

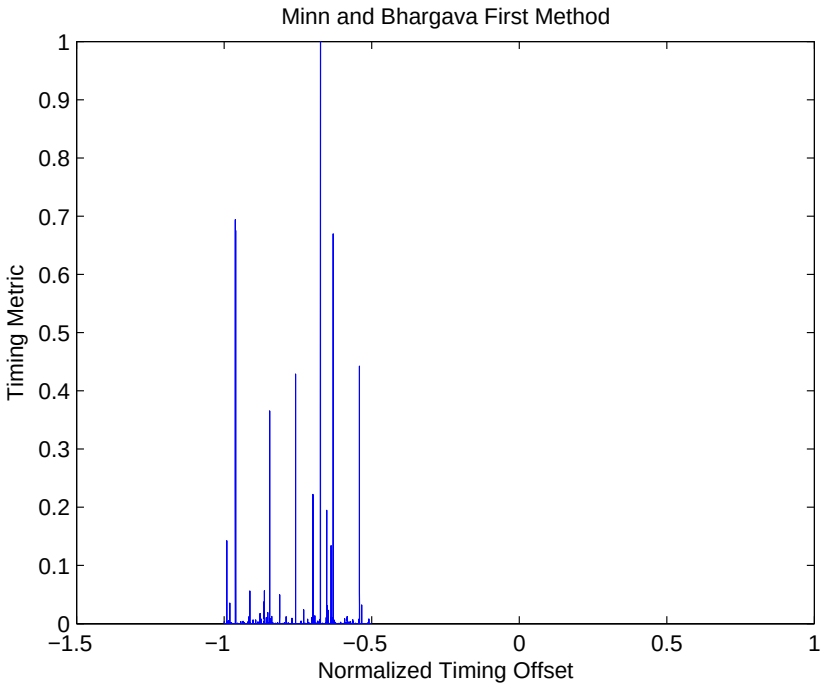

Figure 3.5: Minn and Bhargava's Approach

CHAPTER 4: RESULTS

This chapter presents the results of all the simulations done during the implementation and the performance of DVB-T using OFDM.

4.1 AWGN Environment

The system of OFDM was implemented using DVB-T as an example [24]. To make the analysis more practical, the effect of symbol timing offset was added and investigated. The channel distribution used was Additive White Gaussian Noise (AWGN). We add $4096 - 1705 = 2391$ zeros to the signal *info* to achieve over-sampling and to center the OFDM spectrum. The above operations can be seen in the following figures.

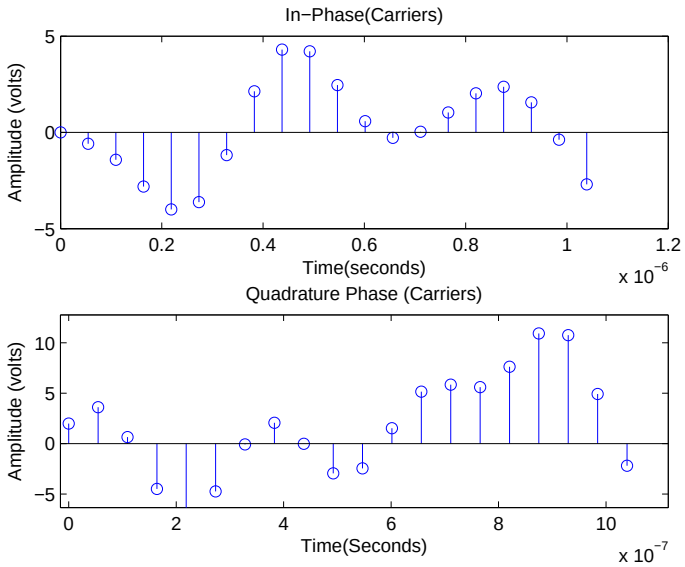

Figure 4.1: Time Response of Signal Carriers

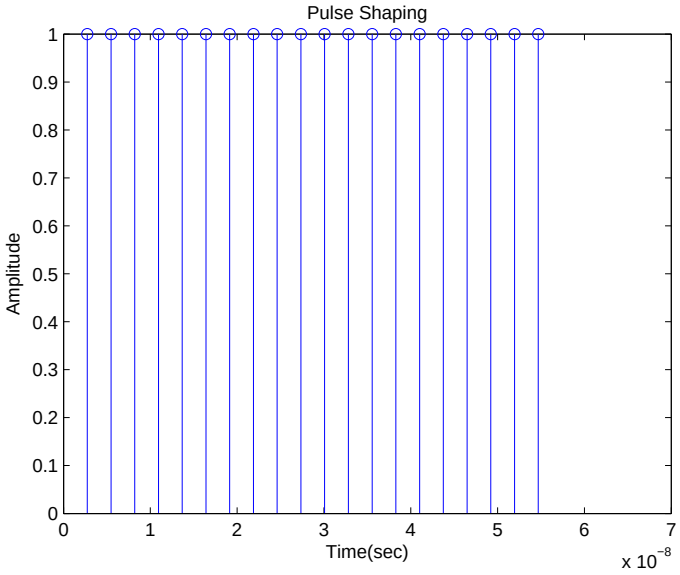

Figure 4.2: Pulse Shape

It is clear that carriers are baseband discrete-time and we can use them for discrete-time baseband simulation. However, the focus of this implementation was on passband continuous time-domain simulation.

The first step to produce a continuous time-domain signal is to apply a transmit filter $g(t)$ whose impulse response is shown in the Figure 4.2.

After using the transmit filter, a reconstruction filter D/A was used to avoid aliasing. The proposed reconstruction filter [24] is a Butterworth filter of order 13 and cut-off frequency of approximately $1/T$. The D/A filter response is shown in the Figure 4.3.

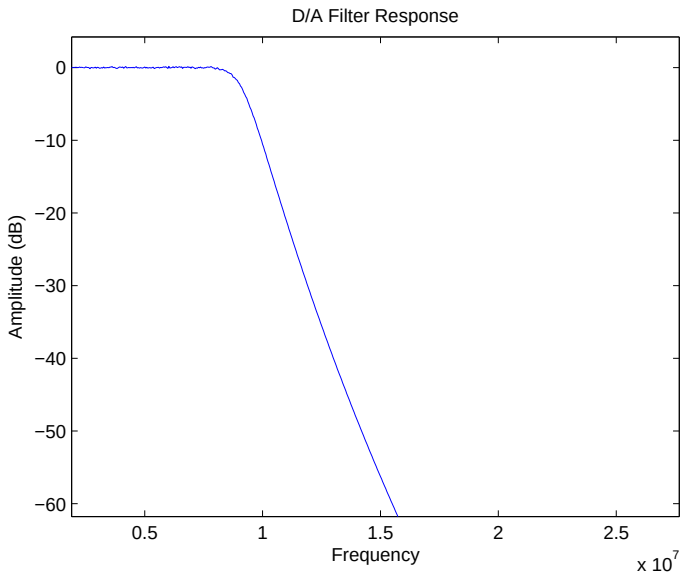

Figure 4.3: D/A Filter Response

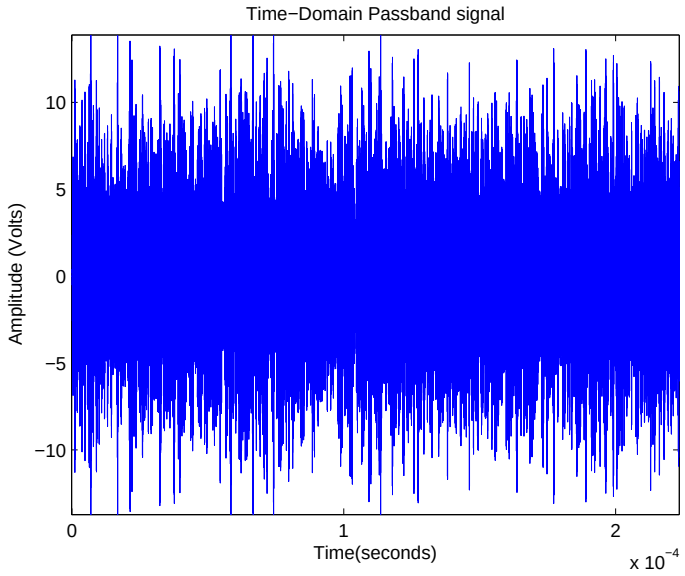

Figure 4.4: Passband Signal

The next step was to perform the quadrature multiplex double-sideband amplitude modulation. In this modulation [25], an in-phase signal $m_I(t)$ and a quadrature signal $m_Q(t)$ are modulated using the formula given below

$$x(t) = m_I(t)cos(2\pi f_c t) + m_Q(t)sin(2\pi f_c t) \tag{4.1}$$

By making the above equation as reference, we can express the emitted signal in (3.1) as

$$x(t) = \sum_{k=K_{min}}^{k=K_{max}} Re(c_{0,0,k}) cos\left[2\pi\left(\left(\frac{k-\frac{K_{max}+K_{min}}{2}}{T_U}+f_c\right)t-\frac{\Delta}{T_U}\right)\right] - \sum_{k=K_{min}}^{k=K_{max}} Im(c_{0,0,k}) sin\left[2\pi\left(\left(\frac{k-\frac{K_{max}+K_{min}}{2}}{T_U}+f_c\right)t-\frac{\Delta}{T_U}\right)\right] \tag{4.2}$$

where we can define the in-phase and quadrature signals as the real and imaginary parts of $c_{m,l,k}$, the 4-QAM symbols respectively. The complete time-domain passband OFDM signal is shown in Figure 4.4.

Figure 4.5 shows the frequency response of the time-domain passband signal as well as power density spectrum of the signal shown over the useful bandwidth.

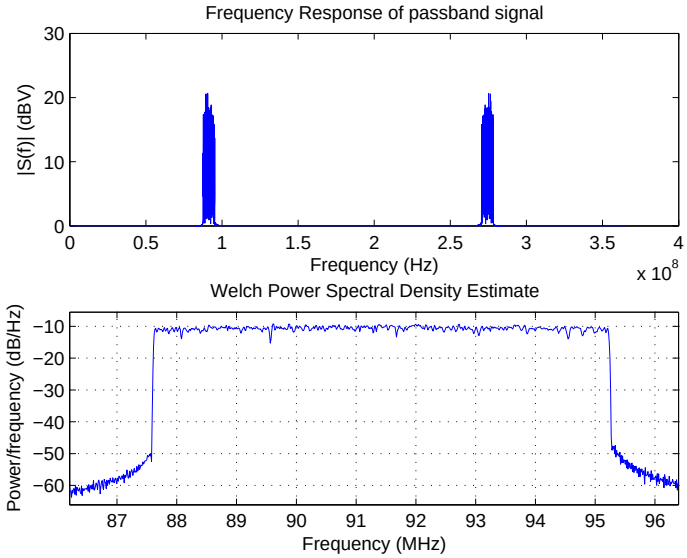

Figure 4.5: Frequency Response of the Passband Signal

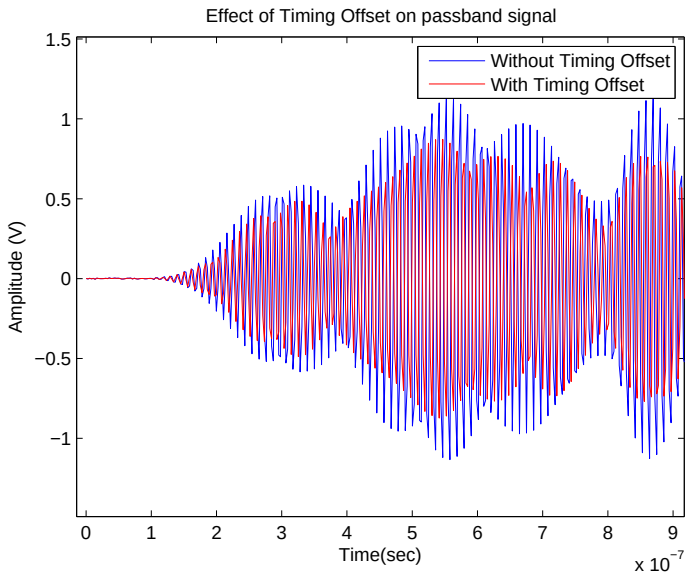

Figure 4.6: Time Response of Signal after Timing Jitter

The effect of timing offset in passband signal can be seen in Figure 4.6 where the comparison between signal with and without time offset is shown.

To observe the effect of timing offset in the system, physical channel information was added. The distribution of channel used was AWGN. The effect of AWGN channel can be seen in Figure 4.7.

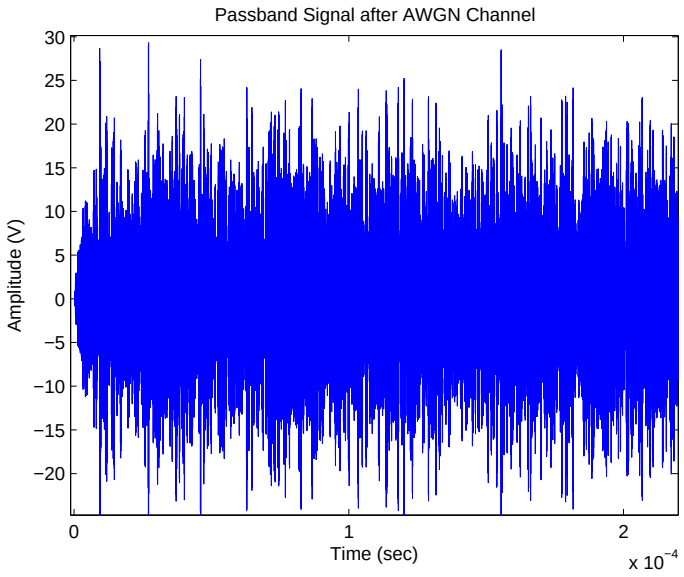

Figure 4.7: Effect of AWGN Channel

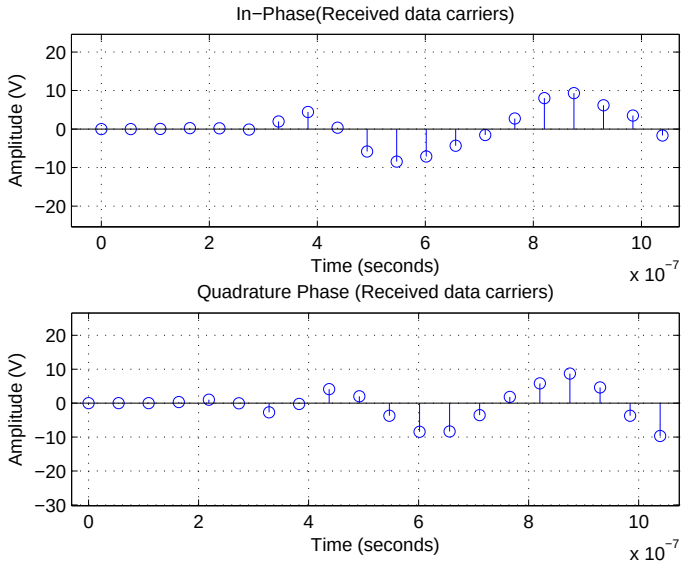

Figure 4.8: Signal Carriers at Receiver

The implementation of receiver was reverse of transmitter. The plot shown in Figure 4.8 shows stem plot of the carriers received at the receiver side. The ideal constellation diagram of a 4-QAM signal is also shown in Figure 4.9.

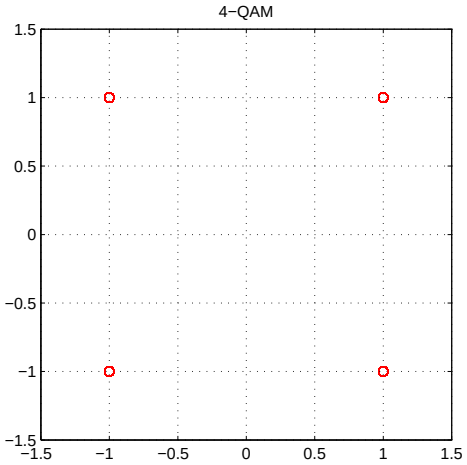

Figure 4.9: Ideal Constellation Diagram

In this study, the sampling rate is $T_s = 2.747ns$ and the time offset was measured by the number of samples delayed. Hence, the actual delay can be calculated using $T_d = kT_s(ns)$, where k is the number of samples delayed.

4.1.1 Case-I (Time Offset=1 sample)

With the time offset value corresponding to 1 sample delayed, simulation was performed to observe the reconstructed signal constellation and the results are as follows:

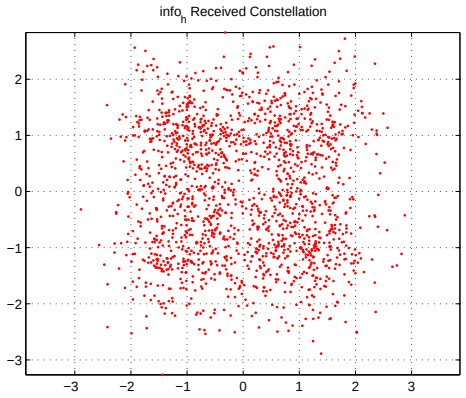

Figure 4.10: Reconstructed Signal Constellation with SNR=0 dB

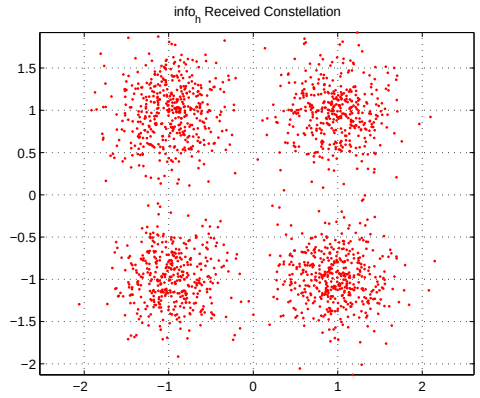

Figure 4.11: Reconstructed Signal Constellation with SNR=6 dB

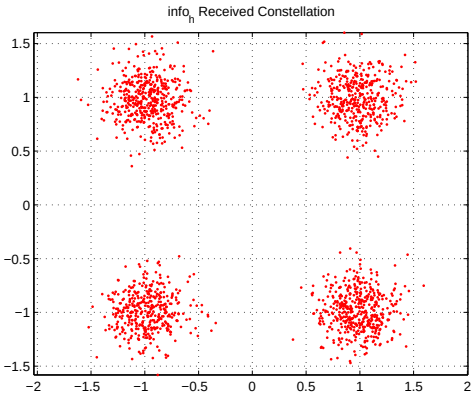

Figure 4.12: Reconstructed Signal Constellation with SNR=12 dB

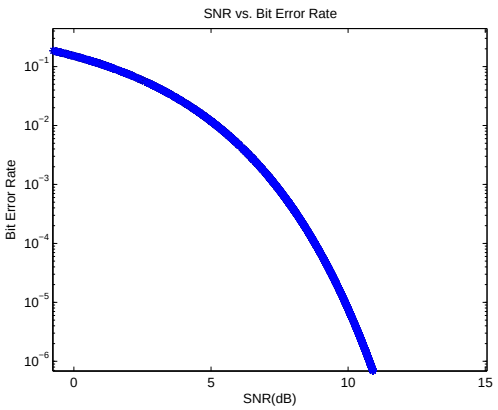

Figure 4.13: Bit Error Rate with Time offset=1 sample

With the time offset corresponding to 1 sample, it is clear that reconstructed signal constellation with higher SNR value follows the ideal constellation more closely than those with less SNR value. It almost require the SNR of 9.8 dB to correct the bit errors at the level of 10^{-5}.

4.1.2 Case-II (Time Offset=5 sample)

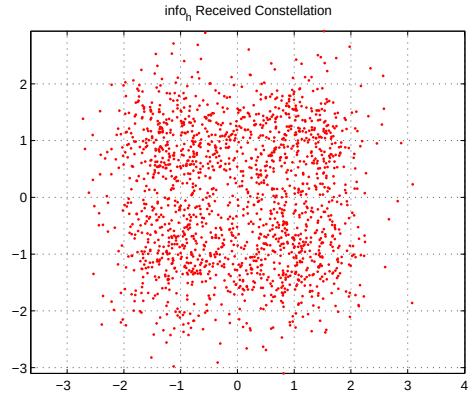

Figure 4.14: Reconstructed Signal Constellation with SNR=0 dB

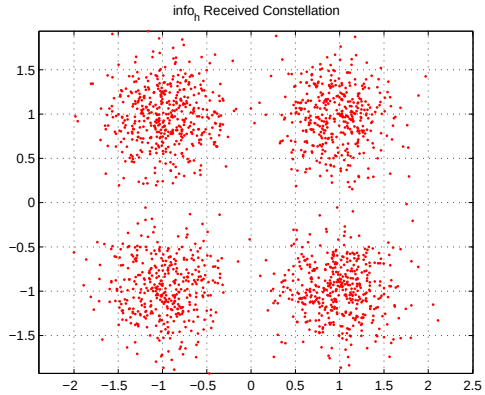

Figure 4.15: Reconstructed Signal Constellation with SNR=6 dB

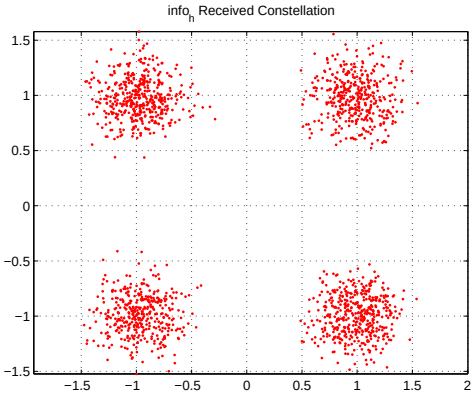

Figure 4.16: Reconstructed Signal Constellation with SNR=12 dB

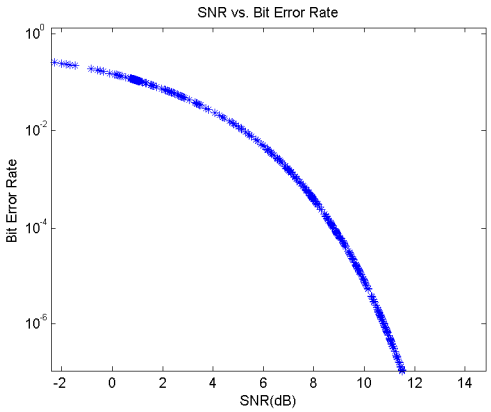

Figure 4.17: Bit Error Rate with Time offset=5 samples

The case II shows the effect of increased timing offset on the reconstructed signal constellation. It requires more SNR than it was needed with timing offset of 1 delayed sample. Also, the SNR value required to correct to the bit error rate at a level of 10^{-5} is also higher than previous case.

4.1.3 Case-III (Time Offset=15 samples)

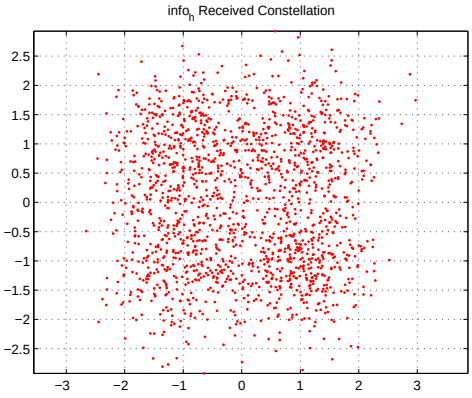

Figure 4.18: Reconstructed Signal Constellation with SNR=0 dB

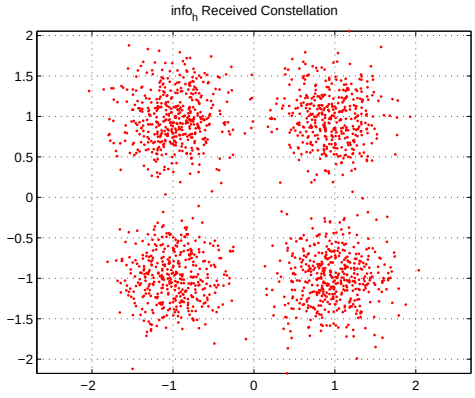

Figure 4.19: Reconstructed Signal Constellation with SNR=6 dB

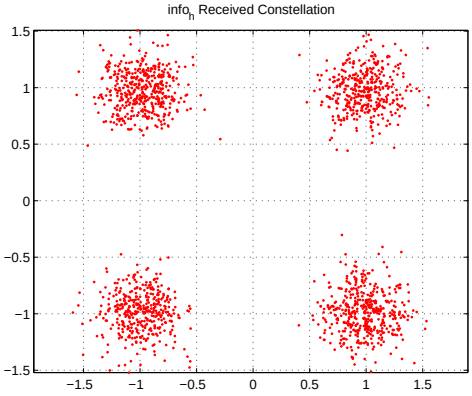

Figure 4.20: Reconstructed Signal Constellation with SNR=12 dB

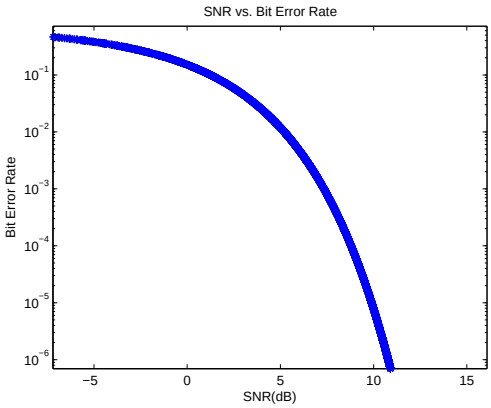

Figure 4.21: Bit Error Rate with Time offset=15 samples

Increasing the delayed samples for timing offset also affects the performance of the system in terms of bit error rate and the trade off can be seen in terms of SNR value of about 10.5 dB.

Table 4.1: Comparison of SNR (dB) versus Timing Offset for AWGN

Timing Offset (samples)	BER	SNR (dB) for AWGN
1	$BER = 10^{-5}$	9.8
5	$BER = 10^{-5}$	10
15	$BER = 10^{-5}$	10.5
30	$BER = 10^{-5}$	10.9

4.1.4 Case-IV (Time Offset=30 samples)

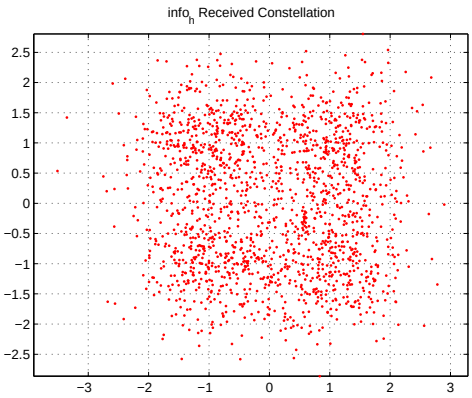

Figure 4.22: Reconstructed Signal Constellation with SNR=0 dB

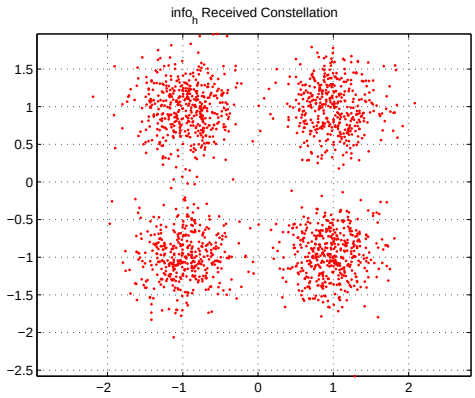

Figure 4.23: Reconstructed Signal Constellation with SNR=6 dB

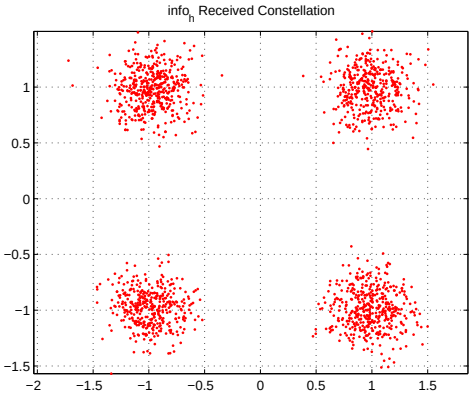

Figure 4.24: Reconstructed Signal Constellation with SNR=12 dB

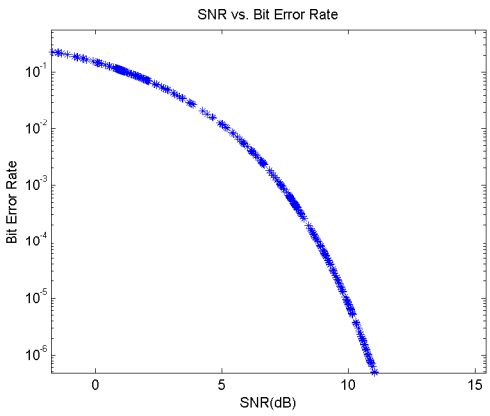

Figure 4.25: Bit Error Rate with Time offset=30 samples

Table 4.1 shows the comparison of timing offset with SNR value in dB. It shows the effect of different timing offset on bit error rate and the SNR required to correct it.

4.2 Rayleigh Fading Environment

The simulations were performed to study the system with Rayleigh Fading Environment. The Rayleigh channel was created by using five delayed signals with different delay values including line of sight. The value of Doppler shift used was 100 and the number of trials were set to 100 too. The bandlimited impulse response of the channel was observed by using the visual channel tool in MATLAB. Fading environment put more fading and delay on the signal [26] and it was observed during the simulation.

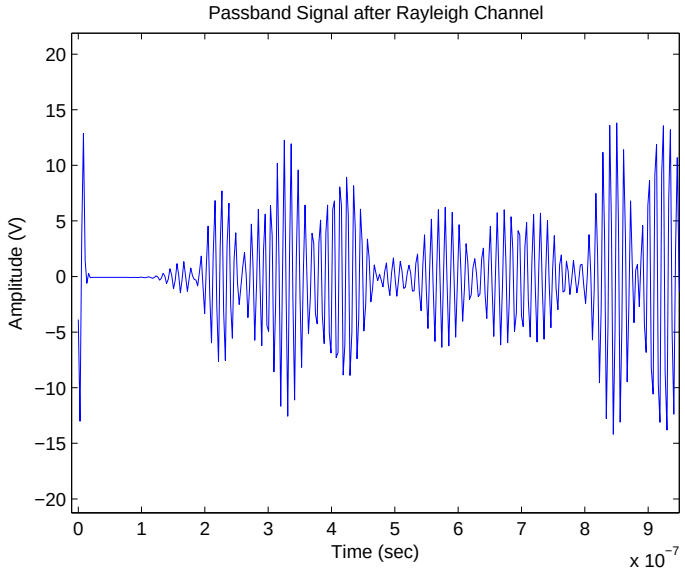

Figure 4.26: Effect of Rayleigh Fading Channel

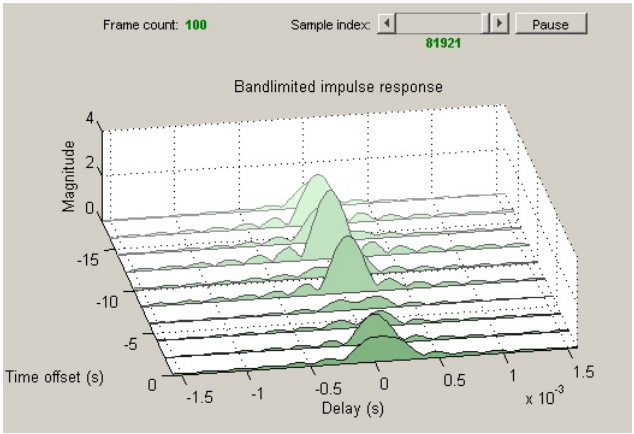

Figure 4.27: Impulse Response of Rayleigh Fading Channel

The impulse response of channel (Figure 4.27) shows the effect of fading with different value of delay and timing offset. It can be seen from the following results that higher SNR (dB)

is required to achieve acceptable bit error rate.

Using the Rayleigh Channel distribution, a comparison was performed to observe the effect of different values of time offset on the received constellation and the results are as follows:

4.2.1 Case-I (Time Offset=1 sample)

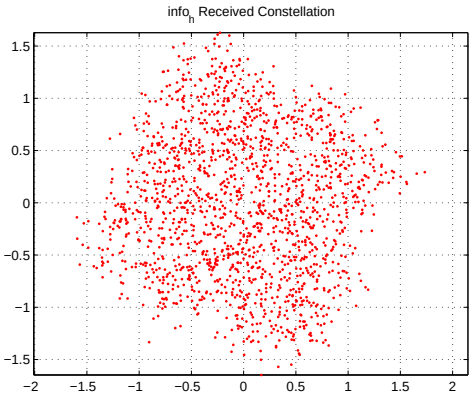

Figure 4.28: Reconstructed Signal Constellation in Rayleigh Environment with SNR=10 dB

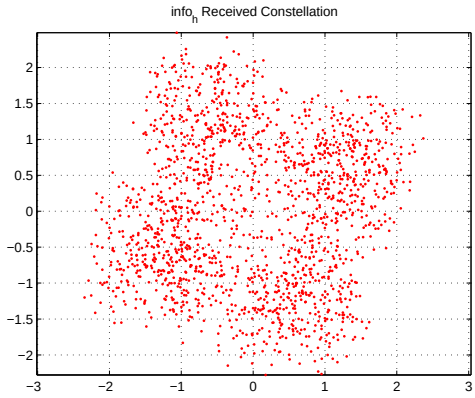

Figure 4.29: Reconstructed Signal Constellation in Rayleigh Environment with SNR=35 dB

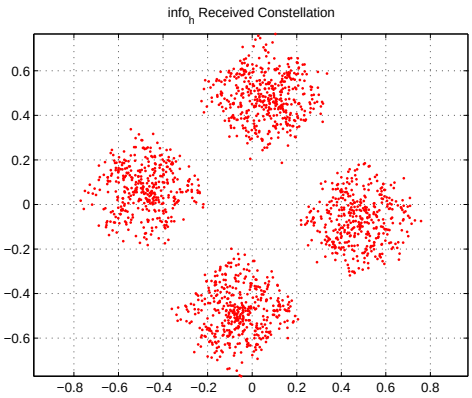

Figure 4.30: Reconstructed Signal Constellation in Rayleigh with SNR=60 dB

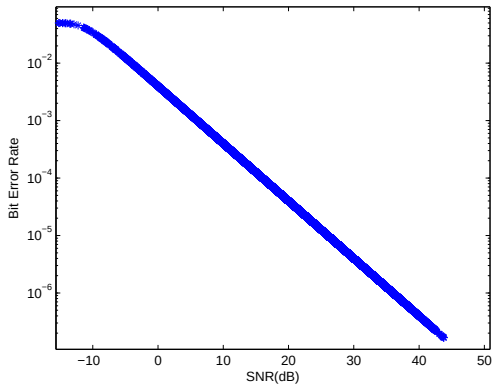

Figure 4.31: Bit Error Rate with Time offset=1 sample in Rayleigh Environment

In Rayleigh environment, the effect of timing offset is more adverse than in AWGN. It requires higher values of SNR to achieve acceptable level of bit error rate for the system in rayleigh

fading environment.

4.2.2 Case-II (Time Offset=5 samples)

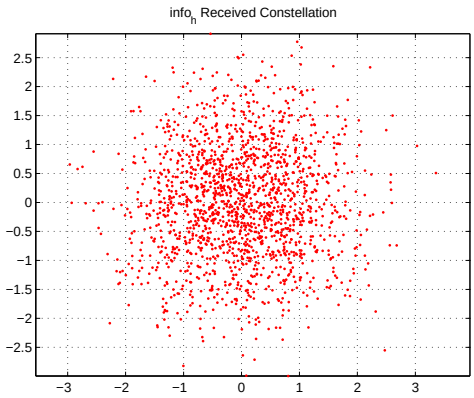

Figure 4.32: Reconstructed Signal Constellation in Rayleigh Environment with SNR=10 dB

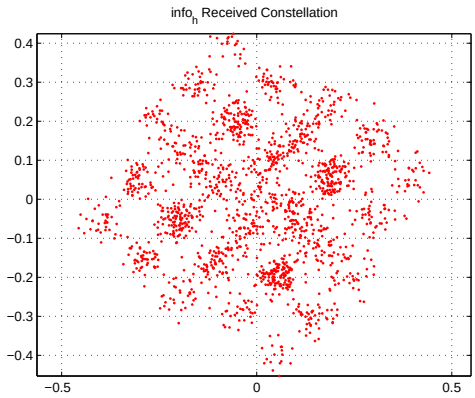

Figure 4.33: Reconstructed Signal Constellation in Rayleigh Environment with SNR=35 dB

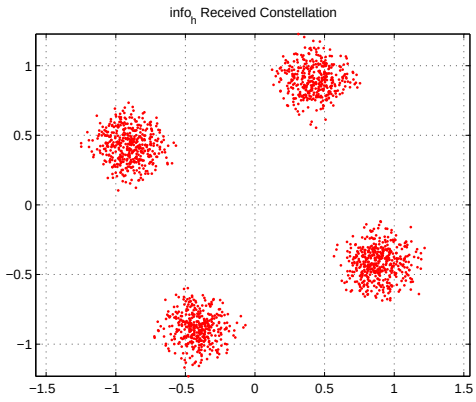

Figure 4.34: Reconstructed Signal Constellation in Rayleigh with SNR=60 dB

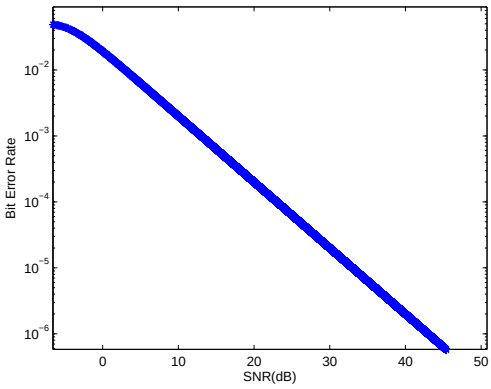

Figure 4.35: Bit Error Rate with Time offset=5 samples in Rayleigh Environment

4.2.3 Case-III (Time Offset=15 samples)

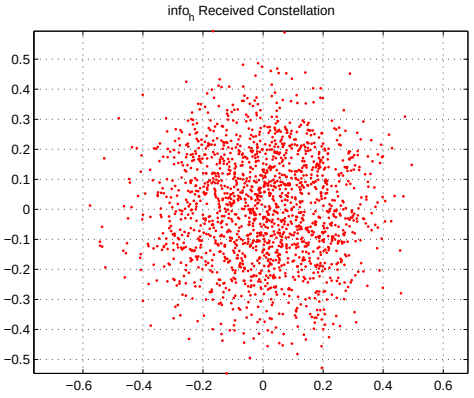

Figure 4.36: Reconstructed Signal Constellation in Rayleigh Environment with SNR=10 dB

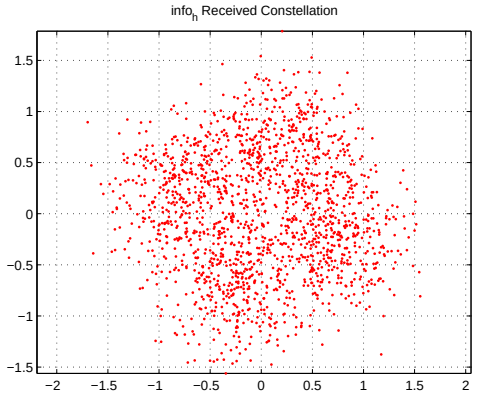

Figure 4.37: Reconstructed Signal Constellation in Rayleigh Environment with SNR=35 dB

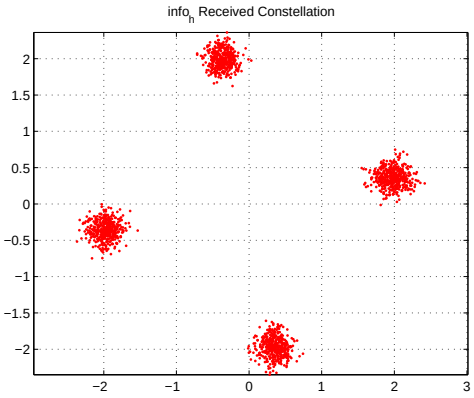

Figure 4.38: Reconstructed Signal Constellation in Rayleigh Environment with SNR=60 dB

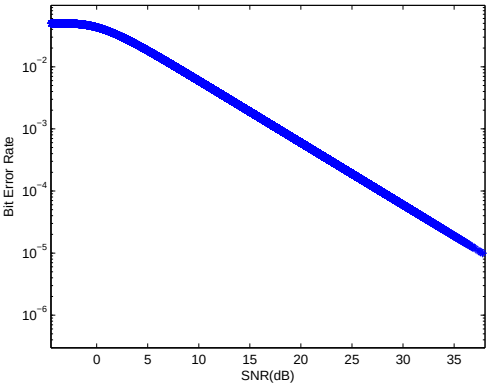

Figure 4.39: Bit Error Rate with Time offset=15 samples in Rayleigh Environment

4.2.4 Case-IV (Time Offset=30 samples)

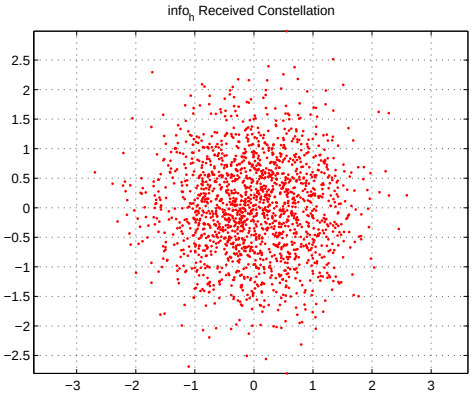

Figure 4.40: Reconstructed Signal Constellation in Rayleigh Environment with SNR=10 dB

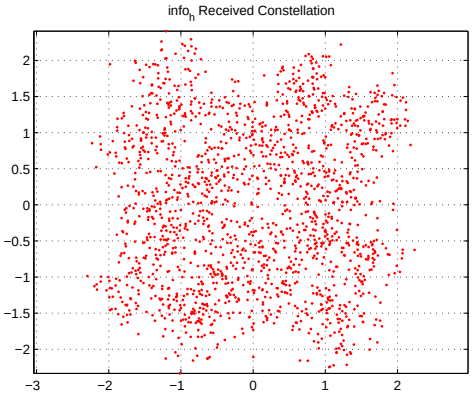

Figure 4.41: Reconstructed Signal Constellation in Rayleigh Environment with SNR=35 dB

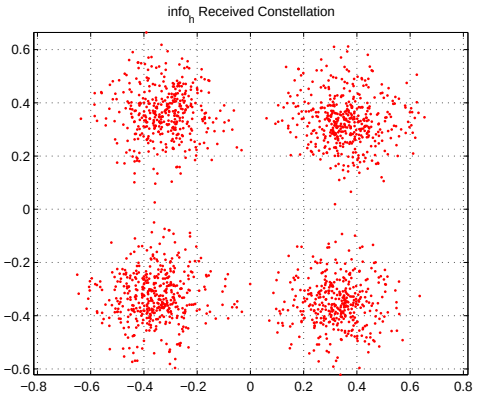

Figure 4.42: Reconstructed Signal Constellation in Rayleigh Environment with SNR=60 dB

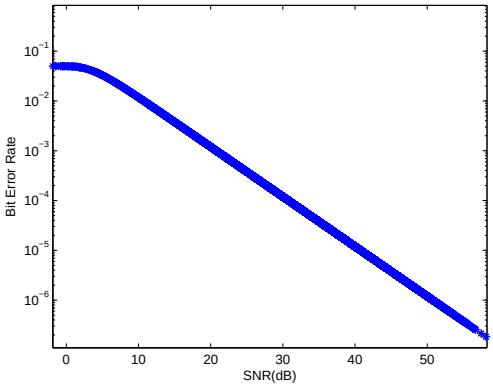

Figure 4.43: Bit Error Rate with Time offset=30 samples in Rayleigh Environment

The reconstructed signal constellations affected by different amount of offset show that there is a phase rotation associated with the constellation. The higher the timing offset, the more scattering and phase shift it will cause to the constellation points. It was also observed that to achieve the acceptable level of bit error rate, the SNR value of almost 40 to 60 dB is required. Table 4.1 shows the comparison of different values of timing offset and the SNR required to correct specified level of BER for Rayleigh environment.

Table 4.2: Comparison of SNR (dB) versus Timing Offset for Rayleigh

Timing Offset (samples)	BER	SNR (dB) for Rayleigh
1	$BER = 10^{-5}$	25
5	$BER = 10^{-5}$	34
15	$BER = 10^{-5}$	40
30	$BER = 10^{-5}$	44

CHAPTER 5: CONCLUSION AND FUTURE WORK

The main objective of this thesis was to study and investigate the need for timing synchronization errors in OFDM system, the major effects of timing offset errors, performance of system with reference to BER and then to compare some of the synchronization algorithms. The goal was achieved by implementing the OFDM system using DVB-T as an example with the effect as well as correction of timing jitter. On the concluding remarks, it was observed that AWGN environment was primitive and good enough to study the topic whereas Fading environment gives the more good picture of practical scenario.

In this thesis, the work was limited to timing offset errors and its correction but there are some suggestions and ideas to be added in future to investigate the OFDM system on more comprehensive level.

5.1 Multiple Input Multiple Output (MIMO)

In a Multiple-Input-Multiple-Output system multiple antennas are used at both the transmitter and receiver to improve communication performance. It is one of several forms of smart antenna technology. MIMO technology has attracted attention in wireless communications, because it offers significant increases in data throughput and link range without additional bandwidth or transmit power. It achieves this by higher spectral efficiency (more bits per second per hertz of bandwidth) and link reliability or diversity (reduced fading). Because of these properties, MIMO is a current theme of global wireless research.

5.1.1 Forms of MIMO

•**Multiple-Input-Single-Output (MISO)** is a degenerate case when the receiver has a single antenna usual transmit diversity configuration.

•**Single-Input-Multiple-Output (SIMO)** is a degenerate case when the transmitter has a single antenna usual receiver diversity configuration.

•**Single-Input-Single-Output (SISO)** is a radio system where neither the transmitter nor receiver has multiple antennas.

•**MIMO** is the case in when both the receiver and the transmitter have multiple antennas.

5.1.2 MIMO Techniques

To achieve MIMO from a conventional SISO system, several technologies have been proposed:

• Beamforming

• Space-time coding/processing

• SDMA

• Spatial multiplexing

The above MIMO technology can be added in the implementation to research the current issue with more details.

5.2 Software Defined Radio (SDR)

After the recent development of new frequency bands, modes and services to wireless communication, there is a need to put all those new modes and services to one respective radio. In other words, each new mode requires its own radio and baseband chipset stuffed into device with single packaging [27]. SDR devices make use of general computational architecture such as FPGAs, DSPs, General purpose CPUs to perform the baseband operations instead of specific hardware (ASICs) [28].

5.3 4G

Another technology to add in future in the research is 4G. OFDM is used in 3G and 4G communication and it is important to investigate the performance of OFDM in these technologies. 4G includes two standards namely Long Term Evolution(LTE) and WiMax Mobile. LTE employs MIMO-OFDM in downlink and Single Carrier Frequency Division Multiple Access (SC-FDMA) [29].

BIBLIOGRAPHY

[1] M. Doelz, E. Heald, and D. Martin, "Binary data transmission techniques for linear systems," *Proceedings of the IRE*, vol. 45, no. 5, pp. 656–661, 1957.

[2] Robert W. Chang, "Synthesis of band-limited orthogonal signals for multichannel data transmission," *Bell Systems Technical Journal*, vol. 45, pp. 1775–1796, Dec. 1966.

[3] M. Okada, S. Hara, and N. Morinaga, "Wideband indoor radio system using orthogonal multicarrier modulation," in *IEEE International Conference on Systems Engineering*, 1992, pp. 457–462.

[4] S.N. Diggavi, "Analysis of multicarrier transmission in time-varying channels," in *IEEE International Conference on Communications*, 1997, vol. 3, pp. 1191–1195.

[5] S. Gifford, John E. Kleider, and S. Chuprun, "Ofdm transmitter power amplifier and par reduction performance: measurement and simulation," in *Proc. MILCOM*, 2002, vol. 1, pp. 591–595.

[6] X. Cui and D. Yu, "Digital ofdm transmitter architecture and fpga design," in *The 8th IEEE International Conference on ASIC (ASICON)*, 2009, pp. 477–480.

[7] R.L. Olsen and T. Tjelta, "Worldwide techniques for predicting the multipath fading distribution on terrestrial LOS links: background and results of tests," *IEEE Transactions on Antennas and Propagation*, vol. 47, no. 1, pp. 157–170, Jan. 1999.

[8] M. Khurram and S.H. Mirza, "A general purpose processor based ieee802.11a compatible ofdm receiver design," in *IEEE GCC Conference*, 2006, pp. 1–5.

[9] Y. S. Cho, *MIMO-OFDM wireless communications with MATLAB*, IEEE Press : J. Wiley & Sons (Asia), Singapore; Hoboken, NJ, 2010.

[10] T.M. Schmidl and D.C. Cox, "Robust frequency and timing synchronization for OFDM," *IEEE Transactions on Communications*, vol. 45, no. 12, pp. 1613–1621, Dec. 1997.

[11] U. Tureli, Hui Liu, and M.D. Zoltowski, "A high efficiency carrier estimator for ofdm communications," in *The Thirty-First Asilomar Conference on Signals, Systems and Computers*, 1997, vol. 1, pp. 505–509.

[12] D.W Lim, S.J. Heo, and J.S. No, "An overview of peak-to-average power ratio reduction schemes for OFDM signals," *Journal of Communication and Networks*, vol. 11, no. 3, pp. 229–239, June 2009.

[13] S.H. Muller and J.B. Huber, "A novel peak power reduction scheme for ofdm," in *The 8th IEEE International Symposium on Personal, Indoor and Mobile Radio Communications*, 1997, vol. 3, pp. 1090–1094.

[14] X. Wang, "Ofdm and its application to 4g," in *The 14th Annual International Conference on Wireless and Optical Communications (WOCC)*, 2005, p. 69.

[15] T. Hwang, C. Yang, G. Wu, S. Li, and G. Ye Li, "OFDM and its wireless applications: A survey," *IEEE Transactions on Vehicular Technology*, vol. 58, no. 4, pp. 1673–1694, May 2009.

[16] IEEE Standard, "802.16.1-2012," Tech. Rep., Sept. 2012.

[17] "IEEE 802.16 published standards and drafts," http://www.ieee802.org/16/published.html.

[18] "IEEE 802.11, the working group setting the standards for wireless LANs," http://www.ieee802.org/11/.

[19] IEEE Standard, "802.11-2007," Tech. Rep., 2007.

[20] H. Minn, M. Zeng, and V.K. Bhargava, "On timing offset estimation for OFDM systems," *IEEE Communications Letters*, vol. 4, no. 7, pp. 242–244, July 2000.

[21] M. Speth, F. Classen, and H. Meyr, "Frame synchronization of ofdm systems in frequency selective fading channels," in *The 47th IEEE Vehicular Technology Conference*, 1997, vol. 3, pp. 1807–1811.

[22] H.A. Harms, L.M. Davis, and J. Palmer, "Understanding the signal structure in dvb-t signals for passive radar detection," in *IEEE Radar Conference*, 2010, pp. 532–537.

[23] European Telecommunication Standards Institute 2004, "Digital video broadcasting (DVB); framing structure, channel coding and modulation for digital terrestrial television," June 2004.

[24] G. Acosta, "OFDM simulation using matlab," Tech. Rep., Georgia Institute of Technology, Smart Antenna Research Laboratory, Aug. 2000.

[25] S. C. Sekhar and T.G Thomas, *Communication Theory*, Electrical and Electronics Series. Mc-Graw Hill, 2006.

[26] P.G. Babalis and C.N. Capsalis, "Impact of the combined slow and fast fading channel characteristics on the symbol error probability for multipath dispersionless channel characterized by a small number of dominant paths," *IEEE Transactions on Communications*, vol. 47, no. 5, pp. 653–657, May 1999.

[27] H.l Yeh and P. Ingerson, "Software-defined radio for ofdm transceivers," in *The 4th Annual IEEE Systems Conference*, 2010, pp. 261–266.

[28] G. Zacheo, D. Djukic, A. Dorni, F. Babich, and F. Ricciato, "A software-defined radio implementation of an 802.11 ofdm physical layer transceiver," in *The 17th IEEE Conference on Emerging Technologies Factory Automation (ETFA)*, 2012, pp. 1–4.

[29] S. Ajey, B. Srivalli, and G. V. Rangaraj, "On performance of mimo-ofdm based lte systems," in *International Conference on Wireless Communication and Sensor Computing (ICWCSC)*, 2010, pp. 1–5.